Traveling and standing wave multipactor measurements

Adrien Plaçais, Eva Al Hajj Sleiman, Julien Angot, Nicolas Faure, Yolanda Gómez Martínez, Thibault Hamelin, Julien Hillairet, Julien Marpaud, Samuel Roni

ONDES AU SERVICE DES PLASMAS
PLASMAS AU SERVICE DES ONDES

Mesures du multipactor en régime stationnaire et progressif
Traveling and standing wave multipactor measurements

Plaçais A.[1], Al Hajj Sleiman E.[2], Angot J.[3], Faure N.[4], Gómez-Mártinez Y.[5], Hamelin T.[6], Hillairet J.[7], Marpaud J.[8], Roni S.[9]

[1]Univ. Grenoble Alpes, CNRS, Grenoble INP, LPSC-IN2P3, 38000 Grenoble France, placais@lpsc.in2p3.fr
[2]CEA, IRFM, 13108 Saint-Paul-lez-Durance, France, eva_sleiman@outlook.com
[3]Univ. Grenoble Alpes, CNRS, Grenoble INP, LPSC-IN2P3, 38000 Grenoble France, angot@lpsc.in2p3.fr
[4]CEA, IRFM, 13108 Saint-Paul-lez-Durance, France, nicolas.faure@cea.fr
[5]Univ. Grenoble Alpes, CNRS, Grenoble INP, LPSC-IN2P3, 38000 Grenoble France, gomez@lpsc.in2p3.fr
[6]CEA, IRFU, 91190 Gif-sur-Yvette, France, thibault.hamelin@cea.fr
[7]CEA, IRFM, 13108 Saint-Paul-lez-Durance, France, julien.hillairet@cea.fr
[8]Univ. Grenoble Alpes, CNRS, Grenoble INP, LPSC-IN2P3, 38000 Grenoble France, marpaud@lpsc.in2p3.fr
[9]Univ. Grenoble Alpes, CNRS, Grenoble INP, LPSC-IN2P3, 38000 Grenoble France, roni@lpsc.in2p3.fr

---

multipactor; coaxial waveguide; experimental
multipactor ; guide d'ondes coaxial ; expérimental

Résumé/Abstract

The results of an experimental campaign on the multipactor phenomenon led at LPSC Grenoble, France, are presented. The campaign was carried out on the MULTIPAC test bench, consisting of a 1" 5/8 coaxial waveguide circuit equipped with diagnostics. The goal was to study the transition between travelling, standing and mixed wave propagation as can occur in particle accelerators as well as some nuclear fusion experimental reactors (*tokamaks*). This was achieved by inserting a stub tuner at the exit of the coaxial line to reflect a fraction of the RF power. We study the influence of the propagation configuration on the multipactor and compare our measurements to analytical laws and numerical simulations from previous studies.

Nous présentons ici les résultats d'une campagne expérimentale portant sur le phénomène multipactor menée au LPSC Grenoble. Elle a été réalisée sur le banc de test MULTIPAC, qui est un guide d'onde coaxial 1" 5/8 équipé de diagnostics. L'objectif était d'étudier la transition entre les modes de propagation stationnaire, progressif et hybride, observée dans les accélérateurs de particules ainsi que dans certains réacteurs de fusion nucléaire (*tokamaks*). Pour cela, nous avons introduit un adaptateur d'impédance (*stub*) à la sortie de la ligne coaxiale permettant de réfléchir une partie de la puissance RF. Nous étudions l'influence du mode de propagation sur le multipactor, et comparons nos mesures à des lois analytiques ainsi qu'à des simulations numériques réalisées lors d'études précédentes.

1 Multipactor under Mixed Wave propagation mode

Multipactor is an exponential increase in the electron population, that can appear in Radio-Frequency (RF) systems placed under vacuum. It materializes when residual electrons enter in resonance with the RF field, and their impact energies with the system walls are high enough to emit other electrons *via* electron emission processes. It is generally considered as a deleterious phenomenon. It alters the propagation of the RF field, and the electrons impacting the walls generate a thermal load. It also creates a polluting plasma *via* desorption processes, which can lead to RF breakdowns in the most extreme scenario. In superconducting RF systems such as found in particle accelerators, the heat can create a *quench* which is a brutal loss of superconductivity. Multipactor can appear on a range of RF field amplitudes (or RF powers) delimited by the lower multipactor threshold and the upper multipactor threshold. Multipactor is a concern in several fields, in particular in telecommunication satellites, particle accelerators and some RF heating systems of experimental nuclear fusion reactors (tokamaks). In this study, we focus on the two latter applications where the impedance of the load can vary during operation, altering the electromagnetic configuration in the system and the apparition of the multipactor.

In tokamaks, RF electromagnetic fields are coupled to the fusion plasma to heat it and/or to ensure its stability. The Ion Cyclotron Resonance Heating (ICRH) systems generate a signal of a few tenths of MHz. It propagates in a Traveling Wave (TW) mode through coaxial lines and an antenna transfers the power to the plasma. The impedance of the magnetized plasma may vary, creating a mismatch with the impedance of the antenna. Then, a fraction of the power is reflected through the coaxial line where the electromagnetic configuration becomes Mixed Wave (MW). In particle accelerators, multipactor can appear in accelerating cavities and the couplers feeding them. Accelerating cavities are resonant systems used to transfer electromagnetic energy to the particles, that cross them by bunches. By the moment they are in the cavities, the wave propagates in TW in the feeding couplers. When the bunch leaves the cavity, RF power is reflected by the cavity to the coupler, where it propagates in Standing Wave (SW) mode.

Hence, both ICRH and particle accelerator couplers face different propagation modes. Several numerical and theoretical studies showed that the wave propagation mode influenced the apparition of the multipactor; in this paper, we propose to verify it experimentally. We introduce the MULTIPAC test bench. This experimental setup, still under development, allows measuring multipactor in a coaxial waveguide while controlling the RF wave propagation mode. In Section 2, we cover some of the previous studies on multipactor under MW regime. In Section 3, we present our test bench. In Section 4, we verify that the electric field in the test bench is consistent with our expectations. In Section 5, we confront our multipactor results with the previous studies from Section 2.

2 Previous findings

We define P_f and P_r the forward and reflected RF powers; the reflection coefficient R can be expressed as:

$$R = \sqrt{\frac{P_r}{P_f}} \tag{1}$$

$R = 0$ means that the propagation mode is TW, $R = 1$ that it is SW, $0 < R < 1$ is MW. We also define the (Voltage) Standing Wave Ratio:

$$SWR = \frac{1 + R}{1 - R} \tag{2}$$

2.1 Somersalo scaling law

Somersalo et al. [1] studied the multipactor in a coaxial waveguide operating under SW, TW and MW propagation modes. They used numerical methods to explore the electrons' resonant trajectories, for various input powers and propagation modes. They proposed the following scaling law:

$$P_{MW} \sim \frac{1}{(1+R)^2} P_{TW} \tag{3}$$

Where P_{MW} is the first multipactor threshold under MW and P_{TW} the first multipactor threshold under TW. They also predicted that a second separated multipactor mode appeared as soon as $R > 0$. Its threshold rapidly grows with R and becomes infinite at $R = 1$.

2.2 Perez work

Perez et al. [2] studied the multipactor in transverse electromagnetic mode cylindrical coaxial transmission lines. They numerically solved the electrons' trajectories in the system and took into account the space-charge effects. They focused on the lowest multipactor threshold. According to the value of fd, where f is the RF frequency and d the distance crossed by the particles, they discriminated two cases. When $fd > 7\ \mathrm{GHz} \cdot \mathrm{mm}$, the lowest voltage threshold $V_{mp,\,lower}$ in the SW case is higher than in the TW case. The regions with low electric fields in the SW case tend to trap electrons, where they gain less energy and emit fewer electrons on impact. When $fd < 7\ \mathrm{GHz} \cdot \mathrm{mm}$, however, the value of $V_{mp,\,lower}$ is independent from the propagation mode.

2.3 Al Hajj Sleiman work

Al Hajj Sleiman et al. [3] also studied the apparition of multipactor in coaxial waveguides. Most of the previous works expressed multipactor barriers using forward RF power and reflection coefficient. Computing or deducing the reflection coefficient or the reflected power is not an easy task in nuclear fusion antennas. They showed that at a given RF power, increasing the SWR widened the range of field amplitudes in the system. Hence it increases the probability that, somewhere, the field amplitude is within the multipactor thresholds allowing the phenomenon to locally appear.

3 Experimental setup

3.1 Test bench configuration

The experimental setup under study is pictured in Figure 1. This test bench, still under development, is located at LPSC Grenoble, France. It is a 1.5 m copper 1”5/8 EIA coaxial waveguide. The main feature of this test bench is that it can be used as a resonant system. A stub located at the end of the coaxial waveguide lets us control the amount of reflected power in the waveguide in a controlled way. Hence, we can reach locally higher electric fields while keeping the same RF power source [4]. RF power is produced by a 80 MHz to 1 GHz MT400 Prana amplifier delivering a forward peak power up to 900 W. It is driven by a SM300 Rohde & Schwartz signal generator. Forward and reflected powers are measured by a E4417A Agilent dual-channel power meter located at the exit of the amplifier. A ZX47-50-S+ Mini-Circuits RF power detector is connected to the acquisition system to obtain a synchronous image of the power shape.

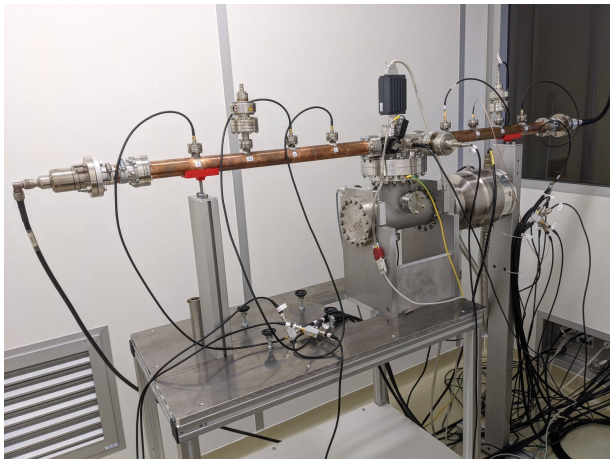

Figure 1: A picture of the test bench in the configuration of the study. The stub is outside of the clean room and is hereby not visible in this picture. Forward RF field propagates from the right to the left of this picture

Two alumina windows are screwed at the extremities of the waveguide. Primary vacuum is ensured by an Agilent Dry Scroll Pump, and secondary vacuum by a Varian TV551 Navigator turbomolecular pump allowing to reach $\sim 10^{-7}$ mbar. The external conductor of the waveguide has several holes called pick-ups to allow the insertion of diagnostics. We verified using ANSYS HFSS that the presence of the pick-ups did not alter in a measurable way the propagation of the wave. The position and name of the pick-ups are represented in Figure 2. At the “V1” and “V3” pick-ups we placed Pfeiffer IKR060 vacuum gauges, and at the “V2” an Agilent Technologies FRG730. They can detect the rise in pressure caused by multipactor desorption processes, allowing for very rapid detection of multipactor apparition. Type K thermocouples from TC S.A. placed at “E1”, “E3”, “E5”, “E7” detect the heat rise due to electrons’ impacts. At the “E” pick-ups we placed home-made RF electric field probes, allowing to know the local magnitude of the electric field. These probes are also electrically biased at + 48 V to collect electrons from the electron cloud and measure DC multipactor current. These probes are essential in this study, as they let us know the value of the electric field and the presence of multipactor from a local perspective.

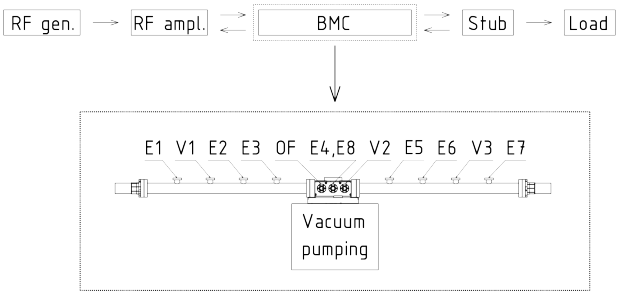

Figure 2: Scheme of the test bench. Forward RF field propagates from the left to the right of the picture

All signals are acquired by a cDAQ-9174 National Instruments chassis. Thermocouple signals are digitized thanks to a NI9211 module. Field probe and current probe signals are digitized by NI9201 analog input modules. We treat all the results with a Python library of tools, under continuous development [5].

3.2 Experimental procedure

The forward RF power was steadily increased up to a maximum, then steadily reduced back. For every test, the power limits are calculated so that most of the pick-ups see the multipactor barrier and cross it. The power cycle is performed several times to condition the surfaces and make different tests comparable. Duration of a full power cycle is approximately 10 min. We will present here our first tests, realized at 120 MHz. We found the stub tunings for objective *SWR* of 1, 2, 4, 10 and $SWR \rightarrow +\infty$ (short-circuit), *SWR* being measured with the power meter. Once all the stub tunings were found, we applied them to perform the tests. Optical fibre for light emission detection and thermocouples diagnostics were not installed at the moment of the tests. We will not consider the signals from the pressure probes in this study; due to hysteresis, the interpretation of their signal requires deeper discussion. All the multipactor thresholds that we present are the ones measured during the last power cycle.

4 Studies on the electromagnetic configuration in the test bench

4.1 Reflected power and SWR

We verified that the *SWR* was constant during the tests and matched our objective values. We calculate it from the measured P_f and P_r for every time step of the tests. We represented it as a function of the measurement index in Figure 3.

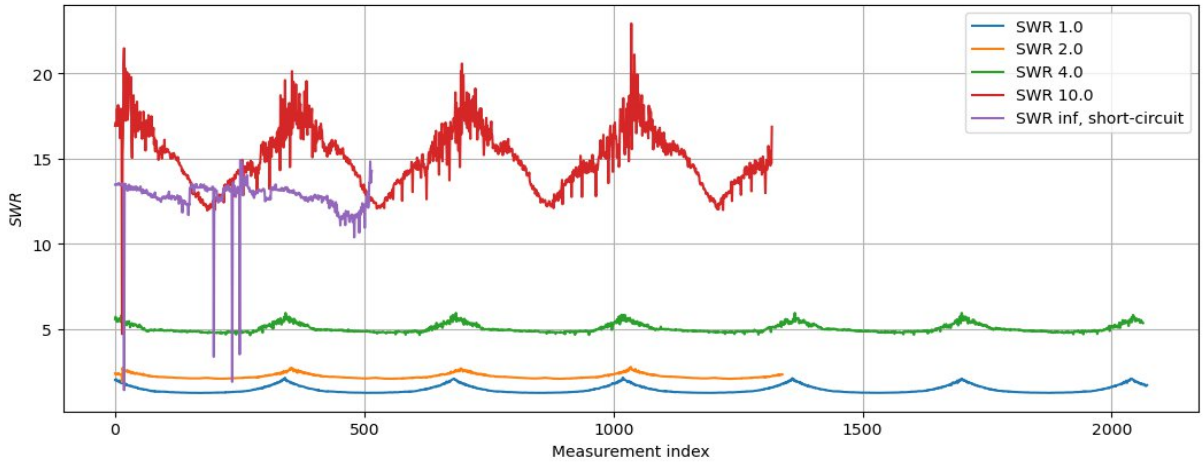

Figure 3: Evolution of Voltage Signal Wave Ratio during the tests.

We can notice that the *SWR* is not constant over the test, and is decreased when the injected power grows. We see three reasons for that. First of all, the RF amplifier's forward power is perturbed by the reflected power. In particular, this is what happens in the short-circuit test, with the amplifier periodically shutting down. The second reason is that the presence of one or several multipactor clouds will reflect a fraction of the power in an

uncontrolled way. Finally, the full propagation chain from the source to the load may be non-linear and depend on the amplitude of the field. Additional RF measurements as well as the introduction of an RF circulator to avoid power return to the source are planned. We note that variations are however relatively low for the tests with $SWR \in [2.0, 4.0]$. For $SWR = 10.0$, they are more significant. The actual values for the *SWR* are summed up in Table 1.

Theoretical *SWR*	Min *SWR*	Mean *SWR*	Max *SWR*	Standard deviation	Relative Standard Deviation [%]
1.0	1.22	1.43	2.13	0.22	15.38
2.0	1.88	2.20	2.76	0.14	6.36
4.0	4.61	5.01	5.93	0.24	4.79
10.0	4.69	15.00	22.93	1.77	11.80
$\rightarrow +\infty$	1.39	12.76	14.92	12.76	100.00

Table 1: SWR data calculated from measured forward and reflected powers

4.2 Consistency of the electric fields measured by the electric field probes

We verified that the electric field measured by the electric field probes matched the analytical law:

$$V_{coax}(z) = V_f \sqrt{1 + R^2 + 2R\cos(2\beta z + \psi_0)} \tag{4}$$

where R is calculated at every measurement point from P_f and P_r, $\beta = c/f$ and ψ_0 is a phase controlling the position of the electric field nodes. Forward voltage V_f is obtained from:

$$V_f = 2\sqrt{P_f Z_0} \tag{5}$$

The line impedance is $Z_0 = 50\ \Omega$. We fitted ψ_0 for the various tests so that the V_{coax} measured by the probes at their position is as close as possible to the V_{coax} calculated from the measured powers. The field probe located at the "E1" pick-up ($z = 0$ m) measured unreasonably high voltages so we excluded its data from the fit. We represented in Table 2 the ψ_0 that we obtained for every test, as well as the value of the coefficient of determination r^2.

Theoretical *SWR*	ψ_0 [rad]	r^2
1.0	3.3	0.962
2.0	3.2	0.961
4.0	3.4	0.979
10.0	3.9	0.989
$\rightarrow +\infty$	1.6	0.841

Table 2: Spatial phase obtained by fitting and r^2 determination coefficient of the fit for the different tests.

Results are satisfactory for all tests but the short-circuit. We also note that r^2 is less satisfactory for the low *SWR* tests. We represented in Figure 4 the voltages measured by the probes for several tests and forward powers (stems) and obtained by fitting analytical law (solid line). For the $SWR = 1.0$, we expect an horizontal line as the electric

field should be uniform in the system. This is what is measured by the electric field probes. However, as we measured a non-null reflected power, the *SWR* that we used for the fit is higher than unity and the fitted law is wave-shaped. Hence, the measure of the reflected power and the *SWR* are overestimated.

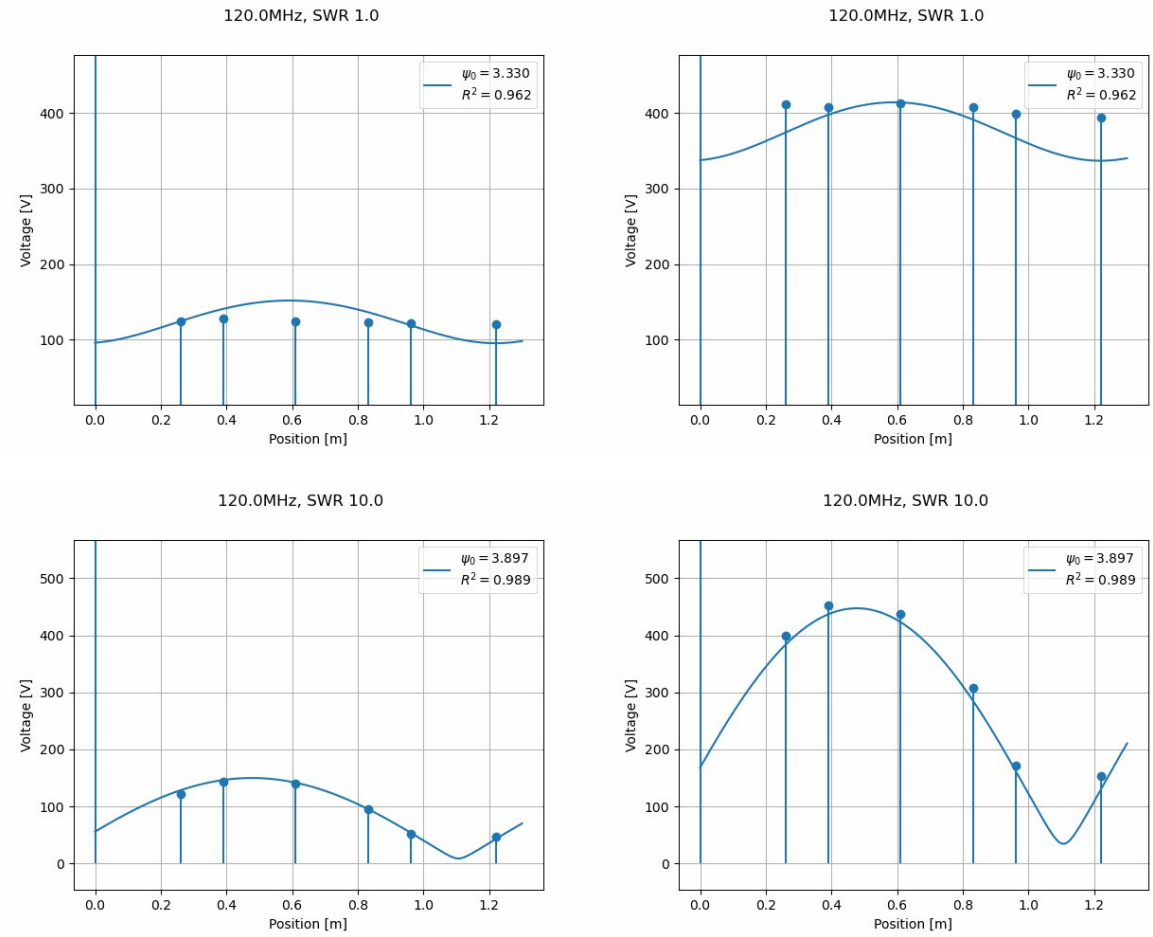

Figure 4: Voltage as a function of position for the $SWR = 1.0$ *(top) and* $SWR = 10.0$ *tests (bottom). Left images are taken at low power and right images at high power. Stems represent the voltage measured by the probes, and solid line the voltage obtained from Equation (4). The field probe "E1" at* $z = 0$ *was not considered for the fit.*

5 Multipactor studies

For this series of tests, we state that a multipactor event occurred when a current probe measured a current above 12 μA. We post-processed the current data to filter out the local bursts and drops of measured current. We excluded the "E1" probe from our process, as the voltage measured at this probe was unreasonably high.

5.1 Somersalo scaling law

For every test, we took the lower power threshold measured during the last power cycle. We also took the value of *R* at the corresponding time step and reported those in Figure 5. We fitted the Somersalo scaling law given by Equation (3); the short-circuit test was excluded from the fit.

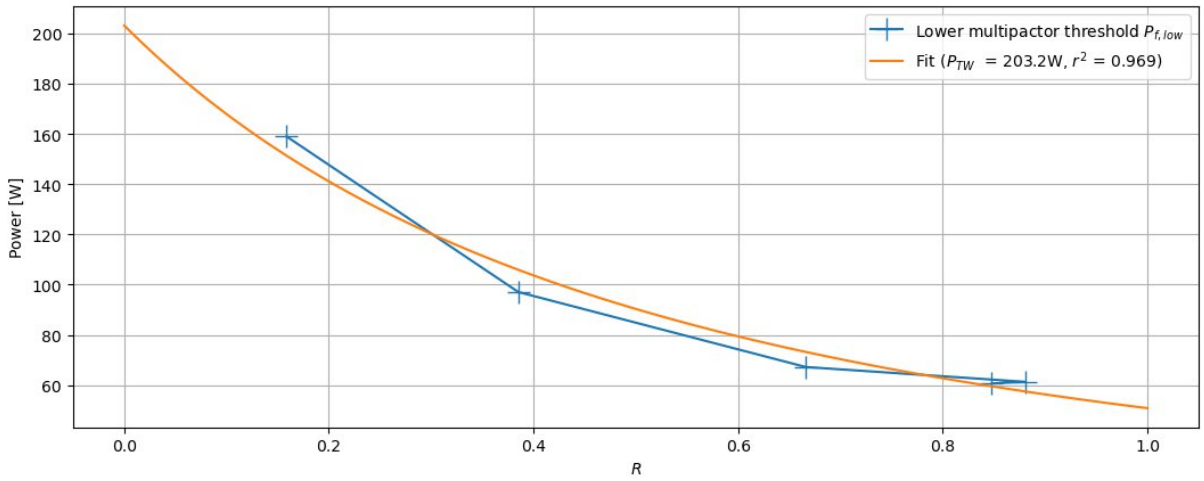

Figure 5: Evolution of the lower multipactor threshold as a function of R, as measured (blue) and with the fitted Somersalo scaling law

We can observe the global tendency for the lower power threshold to be respected. However, we found during post-processing that the test bench was not fully conditioned at the end of the tests, limiting the scope of these conclusions. We did not observe a second multipactor mode at higher powers.

5.2 Checking Perez law

In our configuration, the product fd is $1.3\ \text{GHz} \cdot \text{mm}$, so we expect the lower voltage threshold to be a constant. Similarly to the Somersalo study, we took the lower threshold measured during the last power cycle for every test. Here, the study is local, *i.e.* we discriminate the multipactor according to where it was measured. The voltages are the ones measured by the field probes. We reported it in Figure 6, along with the upper voltage thresholds.

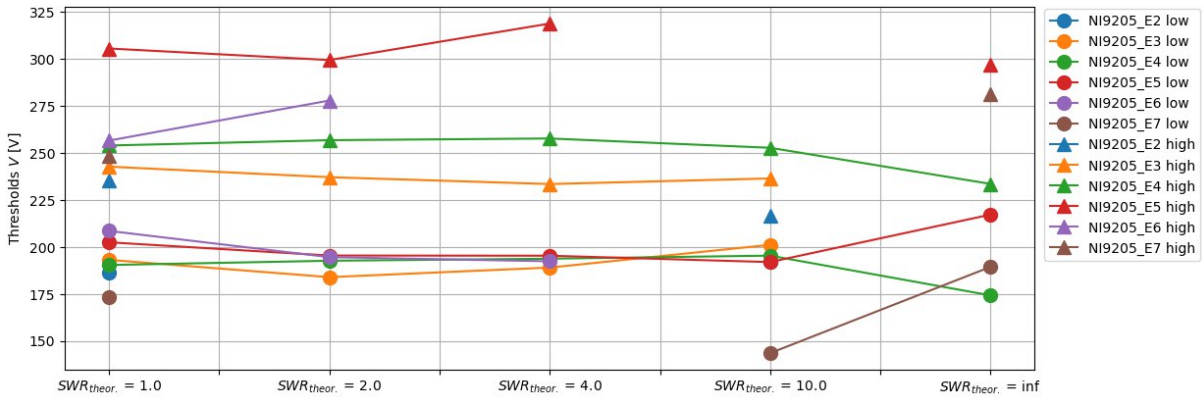

Figure 6: Lower (circles) and upper (triangles) multipactor thresholds measured at every pick-up for every multipactor test

Over all the tests, the mean of the lower thresholds is 191 V with a standard deviation of 14 V, so the relative standard deviation is 7%. The lower threshold, when it is found, exhibits few variations from one test to another and from one pick-up to another — the short-circuit test being an exception. Also, a multipactor at a very low voltage is observed during the $SWR = 10.0$ test at the E7 pick-up. We attribute it to insufficient conditioning. In every test, multipactor was observed at the "E2" probe. However, it was eventually conditioned and there was no multipactor during the last power cycle at this pick-up in all tests but the first.

The mean of the upper multipactor thresholds is 260 V, with a standard deviation of 29 V. The relative standard deviation is 11%, which is close to what we found for the lower threshold. At a given pick-up, the upper threshold varies very little. We think that the differences between the different pick-ups are caused by local variations of electron emission properties and should vanish with a more thorough conditioning. These results suggest that, similar to the lower threshold, the upper voltage threshold is constant with respect to SWR for our values of fd.

6 Conclusions

In this study, we presented our test bench under development. It can detect the apparition of the multipactor in a coaxial waveguide under several propagation modes. First, we confirmed that the electric field measured along the waveguide was consistent with the forward and reflected RF powers. We compared the lower thresholds, in terms of power and voltage, to the work of Somersalo et al. [1] and Perez et al. [2]. They quantitatively match the expected results: the lower power threshold decreases with R, but the lower voltage threshold remains constant. We also observed that the upper voltage threshold varied little with SWR. The scope of our results still suffers from several drawbacks. First of all, we observed a mismatch between the SWR expected by looking at the shape of the electric field and the one that was calculated from P_f and P_r. We plan to fix this by installing a circulator that will avoid the return of power to the RF source. Furthermore, our tests did not last long enough to allow the full conditioning of the bench. Hence, its emission properties may vary from one test to another. As multipactor is extremely sensitive to this parameter, we started a second test campaign with more power cycles. Tests will be performed at different frequencies, allowing us to reproduce and study the susceptibility diagram from Al Hajj Sleiman et al. [3]. Finally, we still have some diagnostics to install and calibrate, in particular the thermocouples. We also plan to develop a Retarding Field Analyzer. This last diagnostic will give us information on the energy of the electrons in the multipactor cloud.

7 Acknowledgements

The authors would like to thank Mohamed Belhaj for his precious help in the development of the test bench and his enlightening comments.

Bibliography

[1] Somersalo, E., Yla-Oijala, P., Proch, D., & Sarvas, J. (1998). Computational methods for analyzing electron multipacting in RF structures. Part. Accel., 59, 107–141. http://cds.cern.ch/record/1120302/files/p107.pdf

[2] Perez, A. M., Tienda, C., Vicente, C., Anza, S., Gil, J., Gimeno, B., Boria, V. E., & Raboso, D. (2009). Prediction of Multipactor Breakdown Thresholds in Coaxial Transmission Lines for Traveling, Standing, and Mixed Waves. IEEE Transactions on Plasma Science, 37(10), 2031–2040. https://doi.org/10.1109/TPS.2009.2028428

[3] Al Hajj Sleiman, E., Hillairet, J., & Belhaj, M. (2022). Multipactor thresholds prediction for geometries subject to standing waves. International Workshop on Multipactor, Corona and Passive Intermodulation in Space RF Hardware (MULCOPIM2022). https://hal.science/hal-03930959

[4] Gómez Martínez, Y., Angot, J., Baylac, M., Cabanel, T., Dumont, P.-O., Emeriaud, N., Longuevergne, D., Sattonnay, G., & Zimmermann, O. (2021). First Measurements on Multipactor Study. 12th International Particle Accelerator Conference, 3633–3635. https://doi.org/10.18429/JACOW-IPAC2021-WEPAB396

[5] Plaçais, A. (2024). MULTIPAC test bench (v1.4.2). https://github.com/AdrienPlacais/multipac_testbench/